



## Research Paper

# The functional significance of redox-mediated intersubunit cross-linking in regulation of human type 2 ryanodine receptor

Roman Nikolaienko<sup>a</sup>, Elisa Bovo<sup>a</sup>, Robyn T. Rebbeck<sup>b</sup>, Daniel Kahn<sup>a</sup>, David D. Thomas<sup>b</sup>, Razvan L. Cornea<sup>b</sup>, Aleksey V. Zima<sup>a,\*</sup>

<sup>a</sup> Department of Cell and Molecular Physiology, Loyola University Chicago, IL, USA

<sup>b</sup> Department of Biochemistry, Molecular Biology and Biophysics, University of Minnesota, Minneapolis, MN, USA



## ARTICLE INFO

## Keywords:

Ca<sup>2+</sup> signaling

Ca<sup>2+</sup> waves

Ryanodine receptor

Sarcoplasmic reticulum and oxidative stress

## ABSTRACT

The type 2 ryanodine receptor (RyR2) plays a key role in the cardiac intracellular calcium (Ca<sup>2+</sup>) regulation. We have previously shown that oxidative stress activates RyR2 in rabbit cardiomyocytes by promoting the formation of disulfide bonds between neighboring RyR2 subunits. However, the functional significance of this redox modification for *human* RyR2 (hRyR2) remains largely unknown. Here, we studied the redox regulation of hRyR2 in HEK293 cells transiently expressing the *ryr2* gene. Analysis of hRyR2 cross-linking and of the redox-GFP readout response to diamide oxidation revealed that hRyR2 cysteines involved in the intersubunit cross-linking are highly sensitive to oxidative stress. In parallel experiments, the effect of diamide on endoplasmic reticulum (ER) Ca<sup>2+</sup> release was studied in cells co-transfected with hRyR2, ER Ca<sup>2+</sup> pump (SERCA2a) and the ER-targeted Ca<sup>2+</sup> sensor R-CEPIA1er. Expression of hRyR2 and SERCA2a produced “cardiac-like” Ca<sup>2+</sup> waves due to spontaneous hRyR2 activation. Incubation with diamide caused a fast decline of the luminal ER Ca<sup>2+</sup> (or ER Ca<sup>2+</sup> load) followed by the cessation of Ca<sup>2+</sup> waves. The maximal effect of diamide on ER Ca<sup>2+</sup> load and Ca<sup>2+</sup> waves positively correlates with the maximum level of hRyR2 cross-linking, indicating a functional significance of this redox modification. Furthermore, the level of hRyR2 cross-linking positively correlates with the degree of calmodulin (CaM) dissociation from the hRyR2 complex. In skeletal muscle RyR (RyR1), cysteine 3635 (C3635) is viewed as dominantly responsible for the redox regulation of the channel. Here, we showed that the corresponding cysteine 3602 (C3602) in hRyR2 does not participate in intersubunit cross-linking and plays a limited role in the hRyR2 regulation by CaM during oxidative stress. Collectively, these results suggest that redox-mediated intersubunit cross-linking is an important regulator of hRyR2 function under pathological conditions associated with oxidative stress.

## 1. Introduction

The type 2 ryanodine receptor (RyR2) is the major sarcoplasmic reticulum (SR) Ca<sup>2+</sup> release channel that plays an essential role in cardiac excitation-contraction (EC) coupling [1,2]. During systole, RyR2 is activated by an inward Ca<sup>2+</sup> current via voltage gated L-type Ca<sup>2+</sup> channels, resulting in global Ca<sup>2+</sup>-induced Ca<sup>2+</sup> release (CICR) [3]. The increase in cytosolic Ca<sup>2+</sup> triggers cellular contraction (systole) followed by a relaxation phase (diastole). During diastole, cytosolic Ca<sup>2+</sup> is pumped back into the SR by the SR Ca<sup>2+</sup>-ATPase (SERCA) and removed outside the cell by Na<sup>+</sup>-Ca<sup>2+</sup> exchanger [4]. Spontaneous RyR2 opening during diastole creates SR Ca<sup>2+</sup> leak that counterbalances SERCA Ca<sup>2+</sup>

uptake and sets SR Ca<sup>2+</sup> load [5,6]. Due to its central role in cardiac function, RyR2 activity is tightly regulated. RyR2 dysfunction, caused either by mutations or stress-induced post-translational modifications, has been linked to various cardiac pathologies, including arrhythmias and heart failure (HF) [7–9].

Among various factors that regulate RyR2 activity, redox modifications of the channel play a particularly important role under pathological conditions associated with oxidative stress [10–12]. Each subunit of the RyR2 homo-tetrameric complex comprises 90 cysteine residues, but only 21 of them are accessible for redox modifications [13,14]. Excessive accumulation of reactive oxygen species (ROS) can cause RyR2 oxidation and increase SR Ca<sup>2+</sup> leak, leading to arrhythmias and

\* Corresponding author. Department of Cell and Molecular Physiology Loyola University Chicago, Stritch School of Medicine, 2160 South First Avenue, Maywood, IL, 60153, USA.

E-mail address: [azima@luc.edu](mailto:azima@luc.edu) (A.V. Zima).

<https://doi.org/10.1016/j.redox.2020.101729>

Received 7 July 2020; Received in revised form 19 August 2020; Accepted 11 September 2020

Available online 15 September 2020

2213-2317/© 2020 The Authors.

Published by Elsevier B.V. This is an open access article under the CC BY-NC-ND license

(<http://creativecommons.org/licenses/by-nc-nd/4.0/>).

contractile dysfunction [15–18]. It has been shown that ROS activate RyR2-mediated  $\text{Ca}^{2+}$  release by promoting spontaneous  $\text{Ca}^{2+}$  sparks [19,20] and  $\text{Ca}^{2+}$  waves [21]. In failing heart, RyR2 oxidation and aberrant SR  $\text{Ca}^{2+}$  release have been linked to the dissociation of the RyR2 regulator calmodulin (CaM) but not FKBP12.6 [22,23]. Despite its clinical significance, the molecular mechanisms of redox regulation as well as the redox-sensitive sites within human RyR2 (hRyR2) remain largely unknown.

The effect of oxidative stress on RyR structure and function is better described for its skeletal muscle isoform (RyR1). It has been shown that only a few cysteines within the RyR1 complex undergo redox modifications [24,25]. Cysteine 3635 (C3635) is considered to be the most important residue responsible for redox regulation of RyR1. This cysteine is localized within the CaM binding domain and can be involved in the channel's regulation by CaM [26–28]. It has been shown that during oxidative stress C3635 can undergo S-nitrosylation, S-glutathionylation or can be oxidized to a disulfide leading to intersubunit cross-linking [26]. Similarly to RyR1, the cardiac RyR2 is also prone to cross-linking during oxidative stress [29]. We have shown previously that this post-translational modification has a profound effect on SR  $\text{Ca}^{2+}$  leak during oxidative stress in rabbit cardiomyocytes [18]. However, it remains unclear whether the corresponding cysteine 3602 (C3602) in RyR2 is involved in cross-linking and what the functional consequence of C3602 redox modification might be. It has been shown that the mutation of C3602 to alanine modulates store overload-induced  $\text{Ca}^{2+}$  release by increasing activation and decreasing termination thresholds [30]. Surprisingly, this mutation prevented neither the channel's activation by oxidative stress nor its regulation by CaM.

In the present study, we assessed the functional significance of intersubunit cross-linking in the regulation of hRyR2. We found that redox-mediated hRyR2 cross-linking is a highly effective post-translational modification associated with oxidative stress. The levels of hRyR2 cross-linking positively correlated with an increase in ER  $\text{Ca}^{2+}$  leak and CaM dissociation from the channel. We also re-evaluated the functional significance of C3602, and showed that this residue is not involved in hRyR2 cross-linking. Moreover, C3602 plays only a limited role in hRyR2 regulation by CaM under control conditions and during oxidative stress.

## 2. Materials and METHODS

### 2.1. R-CEPIA1er, mCer-SERCA2a and GFP-hRyR2 expression

Generation of the vector containing mCer-SERCA2a has been previously described [31]. pCMV R-CEPIA1er was a gift from Dr. Masamitsu Iino (Addgene plasmid 58,216; <http://n2t.net/addgene:58,216>; RRID: Addgene\_58,216). The vector encoding hRyR2 cDNA fused to green fluorescent protein (GFP) at the N-terminus was kindly provided by Dr. Christopher George (University of Cardiff). The C3602A hRyR2 (hRyR<sup>C3602A</sup>) mutant was generated by cloning a fragment of wild type hRyR2 (hRyR2<sup>WT</sup>) cDNA containing C3602, in the pBlueScript II SK(+) cloning vector (kindly provided by Dr. Ruben Mestral, Loyola University Chicago). The mutation C3602A was generated using a site-directed mutagenesis kit (Q5 site-directed mutagenesis kit, NEB). Specific primers containing the mutation were used to amplify the whole plasmid containing the hRyR2 fragment. The mutated RyR2 fragment was cloned back into the hRyR2 backbone, yielding the C3602A mutant. After verification of the mutagenesis by single pass analysis, the plasmids were amplified and used for experimentation. For functional measurements, HEK293 cells were grown on 30 mm plastic dishes for 24 h, and co-transfected with three different plasmids containing GFP-hRyR2, mCer-SERCA2a and R-CEPIA1er genes respectively. Transfection was carried out using polyethylenimine (PEI). 24 h after transfection, cells were transferred to laminin-coated Lab-Tex chambers (ThermoFisher Scientific, USA) and grown for another 24 h. Experiments on transfected cells were carried out 48 h after transfection when

expression of the exogenous genes was optimal.

### 2.2. Measurements of RyR2 cross-linking

HEK293 cells were grown on 100 mm plastic dishes for 24 h and then transfected with the GFP-hRyR2 plasmid using PEI. Cells were further grown for another 48 h. Cells were harvested and resuspended in the solution containing (in mM): 150 K-aspartate, 0.25  $\text{MgCl}_2$ , 0.1 EGTA, 10 HEPES, pH 7.2. Cell suspensions were permeabilized with 0.005% saponin for 5 min and incubated with different diamide concentrations for 10 min. The control group was further treated with 5 mM DTT. The treated cells were harvested and resuspended in lysis buffer (150 mM NaCl, 25 mM HEPES pH 7.4, 1% Triton X-100, phosphatases inhibitors) with 5 mM N-ethylmaleimide (NEM) to block free sulfhydryl groups. Lysate samples were incubated with non-reducing Laemmli buffer for 10 min, ran on 2–10% polyacrylamide gradient SDS-PAGE gels and blotted overnight onto the nitrocellulose membrane. Cross-linking was detected using F1 anti-RyR2 primary antibody (1:1000; Santa Cruz, USA) and anti-mouse secondary antibody (1:5000; Santa Cruz, USA). The amount of hRyR2 cross-linking was analyzed in ImageJ software (NIH, USA), based on the disappearance of the monomeric 560kD band.

### 2.3. Generation of the roGFP-PLB sensor

pLPCX redox GFP (roGFP)-ORP1 was provided by Dr. Tobias Dick (German Cancer Research Group, Heidelberg). roGFP cDNA without the STOP codon was amplified and cloned into pCDNA3.1 (ThermoFisher Scientific, USA), obtaining pCDNA3.1-roGFP. pCMV-phospholamban (PLB) was kindly donated by Dr. Seth Robia (Loyola University Chicago, USA). The PLB cDNA was amplified and cloned into the pCDNA3.1-roGFP, after the roGFP cDNA, yielding pCDNA3.1-roGFP-PLB. In this construct, roGFP is fused to the N-terminus domain of PLB. After verification of sequences by single pass analysis (AGCT inc., USA), the roGFP-PLB plasmid was used for experimentation.

### 2.4. Measurements of oxidative stress, $[\text{Ca}^{2+}]_{\text{ER}}$ and CaM-hRyR2 binding

All experiments were conducted using a laser scanning confocal microscope (Radiance 2000 MP, BioRad) equipped with a 40x oil objective lens (N.A. = 1.3). The cells prepared for an experiment were washed with a solution containing (in mM): 150 K-aspartate, 0.25  $\text{MgCl}_2$ , 0.1 EGTA, 10 HEPES, pH 7.2. Then, the plasma membrane was permeabilized with 0.005% saponin dissolved in the experimental solution containing (in mM): K-aspartate 100; KCl 15;  $\text{KH}_2\text{PO}_4$  5; MgATP 5; EGTA 0.35;  $\text{CaCl}_2$  0.22;  $\text{MgCl}_2$  0.75; HEPES 10; dextran (MW: 40,000) 2% and pH 7.2. Free  $[\text{Ca}^{2+}]$  and  $[\text{Mg}^{2+}]$  were 200 nM and 1 mM respectively. After the permeabilization, the cells were perfused with saponin-free solution during an experiment.

The level of oxidative stress at the cytosolic side of the ER membrane was measured with roGFP-PLB. For roGFP excitation, we used the 488-nm line of the argon laser, and signal was collected at >515 nm. 2D images (512 × 512 pixels) were collected every 10 s at a scanning speed of 6 ms/line. As the roGFP fluorescence decreases with the increase of roGFP oxidation, the recorded signal (F) was presented as background-subtracted  $(1 - F/F_{\text{Max}})$  values. The background fluorescence was recorded during the maximum roGFP oxidation with 100  $\mu\text{M}$  diamide. The maximal signal ( $F_{\text{Max}}$ ) was recorded in the presence of 5 mM DTT.

Changes in  $[\text{Ca}^{2+}]_{\text{ER}}$  were recorded with the  $\text{Ca}^{2+}$  sensor R-CEPIA1er in HEK293 cells expressing GFP-hRyR2 and mCer-SERCA2a. R-CEPIA1er was excited with the 543-nm line of a He-Ne laser and fluorescence was measured at >580 nm. For  $\text{Ca}^{2+}$  wave measurements, 2D images (256 × 256 pixels) were collected every 0.5 s at a scanning speed of 2 ms/line. For measurements of ER  $\text{Ca}^{2+}$  load-leak balance, 2D images (512 × 512 pixels) were collected every 5 s at a scanning speed of 6 ms/line. At the end of each experiment, caffeine (10 mM) was applied to induce complete depletion of  $[\text{Ca}^{2+}]_{\text{ER}}$ . Then,  $F_{\text{Max}}$  was estimated by

application of 2  $\mu\text{M}$  ionomycin and 10 mM  $\text{Ca}^{2+}$ . The changes in  $[\text{Ca}^{2+}]_{\text{ER}}$  were presented normalized according to  $[\text{Ca}^{2+}]_{\text{ER}} = (F - F_{\text{min}}) / (F_{\text{max}} - F_{\text{min}})$ .

To measure the CaM dissociation from hRyR2, we used CaM labeled at position 34 with Alexa Fluor 568 C5 maleimide (F-CaM), which was prepared as we previously described [32]. Permeabilized cells expressing GFP-hRyR2 were saturated with 300 nM F-CaM for 10 min, and then were equilibrated in 60 nM F-CaM. The solution in the chamber was replaced by the experimental solution containing diamide (25 or 50  $\mu\text{M}$ ) with F-CaM (60 nM), followed by 10 min incubation. After the subtraction of background fluorescence, the bound F-CaM fluorescence was calculated according to:  $F(\text{F-CaM}) = (F - F_{\text{min}}) / (F_0 - F_{\text{min}})$ .  $F_{\text{min}}$  was obtained after treating cells with suramin (100  $\mu\text{M}$ ) with no F-CaM.

## 2.5. Statistics

All data presented as means  $\pm$  SEM of  $n$  measurements. Obtained 2D images were analyzed using ImageJ software (NIH, USA). Groups were compared using the Student's  $t$ -test for unpaired data sets and differences were considered statistically significant at  $P < 0.05$ . Peak analysis, statistical analysis, and graphical representation of averaged data was carried out on Origin 2016 SR2 software (OriginLab, USA).

## 3. Results

### 3.1. Sensitivity of hRyR2 cross-linking to oxidative stress

We have shown that the thiol-specific oxidant diamide causes disulfide cross-linking between RyR2 subunits in rabbit ventricular myocytes [29]. To characterize the sensitivity of hRyR2 to oxidative stress, cross-linking was measured upon application of increasing concentrations of diamide in permeabilized HEK293 cells expressing GFP-hRyR2. This oxidative treatment led to the formation of hRyR2 high molecular weight oligomeric forms ( $>1$  MDa) together with a gradual disappearance of the monomeric 560 kDa RyR2 band (Fig. 1A). The application of 5 mM reducing agent DTT prevented hRyR2 cross-linking induced by diamide. Changes in the monomeric hRyR2 band density after oxidation was used to quantify the cross-linking level. We found that incubation with 25  $\mu\text{M}$  diamide caused a full disappearance of the monomeric band, yielding 100% hRyR2 cross-linking (Fig. 1D). Next, we analyzed the level of roGFP oxidation at the cytosolic side of ER membrane. The redox sensor roGFP reports the level of oxidation of two cysteines within the

GFP  $\beta$ -barrel [33]. To anchor roGFP to the ER membrane, we fused it to the cytosolic N-terminus of transmembrane protein PLB (Fig. 1B). This led to a similar cellular localization pattern of roGFP-PLB as that of hRyR2 (Fig. 3A), suggesting that the sensor was successfully targeted to the ER membrane. Dose-dependence of roGFP-PLB cysteine oxidation was measured during the application of increasing concentrations of diamide (Fig. 1C). These experiments revealed that 25  $\mu\text{M}$  diamide that produced the maximal hRyR2 cross-linking caused only  $69 \pm 5\%$  ( $n = 11$ ) roGFP-PLB cysteine oxidation and  $>50$   $\mu\text{M}$  diamide was required to fully oxidize this biosensor. We determined that the  $K_M$  of hRyR2 cross-linking and of the roGFP signal were  $6.27 \pm 1.72$  ( $n = 5$ ) and  $16.54 \pm 6.58$   $\mu\text{M}$  ( $n = 11$ ), respectively (Fig. 1D). It appeared that the hRyR2 cysteines involved in the cross-linking are highly sensitive to oxidative stress. Since 25 and 50  $\mu\text{M}$  diamide produced similar hRyR2 cross-linking but different extents of roGFP-PLB oxidation, we analyzed how these two concentrations affect the hRyR2- $\text{Ca}^{2+}$  release and the hRyR2-CaM binding.

### 3.2. Effect of oxidative stress on $\text{Ca}^{2+}$ waves and ER $\text{Ca}^{2+}$ load

Permeabilized HEK293 cells expressing GFP-hRyR2 and mCER-SERCA2a together with the ER  $\text{Ca}^{2+}$  sensor R-CEPIA1er were used to evaluate the effect of diamide on ER  $\text{Ca}^{2+}$  release. Co-expression of hRyR2 and SERCA2a generated periodic  $\text{Ca}^{2+}$  waves due to spontaneous activation of hRyR2 followed by SERCA  $\text{Ca}^{2+}$  reuptake (Fig. 2A; Control), thus providing a cellular model to reproduce "cardiac-like"  $\text{Ca}^{2+}$  release events [31]. Application of 25  $\mu\text{M}$  diamide caused a fast decline of the basal  $[\text{Ca}^{2+}]_{\text{ER}}$  (or ER  $\text{Ca}^{2+}$  load) by  $29.5 \pm 3.4\%$  ( $n = 22$ ) followed by the cessation of  $\text{Ca}^{2+}$  waves. 50  $\mu\text{M}$  diamide resulted in similar functional response and did not produce further decline in  $[\text{Ca}^{2+}]_{\text{ER}}$  (Fig. 2A and B). In the presence of 50  $\mu\text{M}$  diamide, ER  $\text{Ca}^{2+}$  load decreased by  $30.7 \pm 4.2\%$  ( $n = 17$ ). The high frequency of  $\text{Ca}^{2+}$  waves at the 200 nM cytosolic  $[\text{Ca}^{2+}]$  did not allow an accurate measurement of ER  $\text{Ca}^{2+}$  load. Lowering cytosolic  $[\text{Ca}^{2+}]$  to 100 nM abolished  $\text{Ca}^{2+}$  waves, but maintained ER  $\text{Ca}^{2+}$  load at a steady level. We found that 25 and 50  $\mu\text{M}$  diamide produced similar declines in ER  $\text{Ca}^{2+}$  load (Fig. 1 Sup). Since SERCA function is unaffected by these diamide concentrations [31], the decline in  $[\text{Ca}^{2+}]_{\text{ER}}$  was likely mediated by an increase in ER  $\text{Ca}^{2+}$  leak via hRyR2. These results show that the maximal effect of 25  $\mu\text{M}$  diamide on  $\text{Ca}^{2+}$  waves and ER  $\text{Ca}^{2+}$  leak correlates with the maximum level of hRyR2 cross-linking (Fig. 1A), which is consistent with a functional importance of this redox modification. Since these

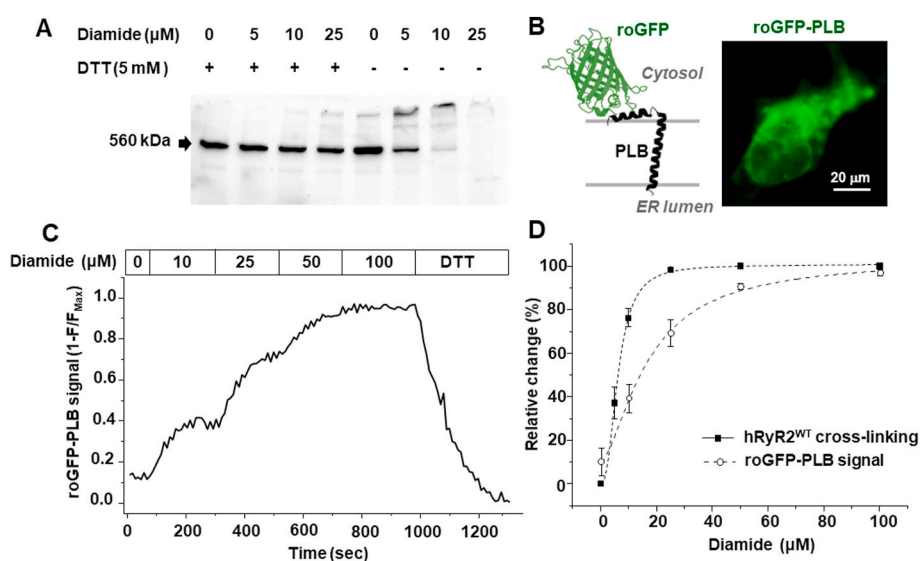


**Fig. 1. Effect of diamide on hRyR2<sup>WT</sup> cross-linking and roGFP-PLB oxidation.** A, Western blot images of hRyR2 cross-linking induced by increasing concentrations of diamide. The control samples were treated with 5 mM DTT to prevent hRyR2 oxidation and cross-linking. B, a schematic diagram of the roGFP-PLB sensor. The redox sensor roGFP was fused to the N-terminus of PLB to measure oxidative stress at the cytosolic side of ER membrane (left). Expression pattern of the roGFP-PLB sensor in HEK293 cells (right). C, changes of the roGFP-PLB signal in response to increasing concentrations of diamide. As the roGFP-PLB signal decreases with an increase of roGFP oxidation, the recorded signal (F) was presented as background-subtracted  $(1 - F/F_{\text{max}})$  values. The background fluorescence was recorded during the maximum roGFP oxidation with 100  $\mu\text{M}$  diamide.  $F_{\text{max}}$  was recorded in the presence of 5 mM DTT. D, dose-dependence of the hRyR2<sup>WT</sup> cross-linking ( $n = 5$  western blots) and the roGFP-PLB signal ( $n = 11$  cells) from diamide concentration. The data were fitted by the Hill equation using the built-in Origin 2016 SR Hill function, which was also used to determine the Michaelis constant ( $K_M$ ).

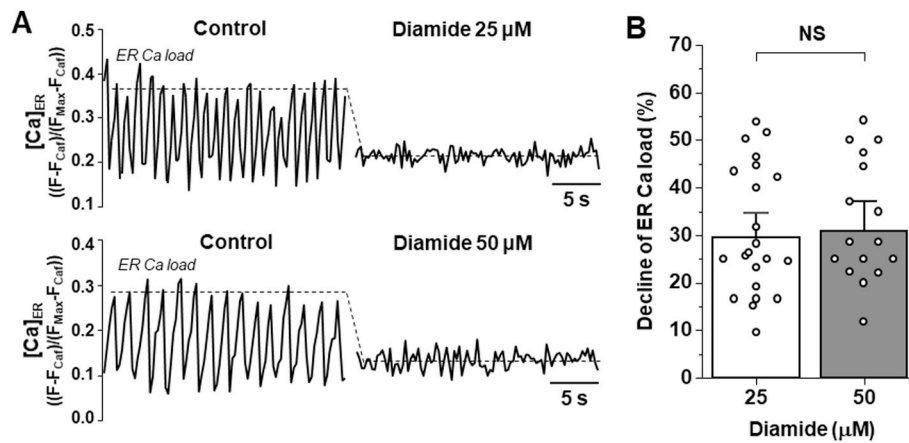


**Fig. 2.** Effects of diamide on hRyR2<sup>WT</sup>-mediated Ca<sup>2+</sup> waves and ER Ca<sup>2+</sup> load. **A**, representative recordings of Ca<sup>2+</sup> waves from two different cells (top and bottom) expressing hRyR2<sup>WT</sup> and SERCA2a in the control conditions (left) and during 25 μM or 50 μM diamide application (right). The dashed lines indicate the level of ER Ca<sup>2+</sup> load. **B**, the effect of diamide on ER Ca<sup>2+</sup> load. ER Ca<sup>2+</sup> load was measured between Ca<sup>2+</sup> waves. On average, changes in ER Ca<sup>2+</sup> load induced by 25 μM (n = 22 cells) and 50 μM (n = 17 cells) diamide were not significantly different (p = 0.82; NS).

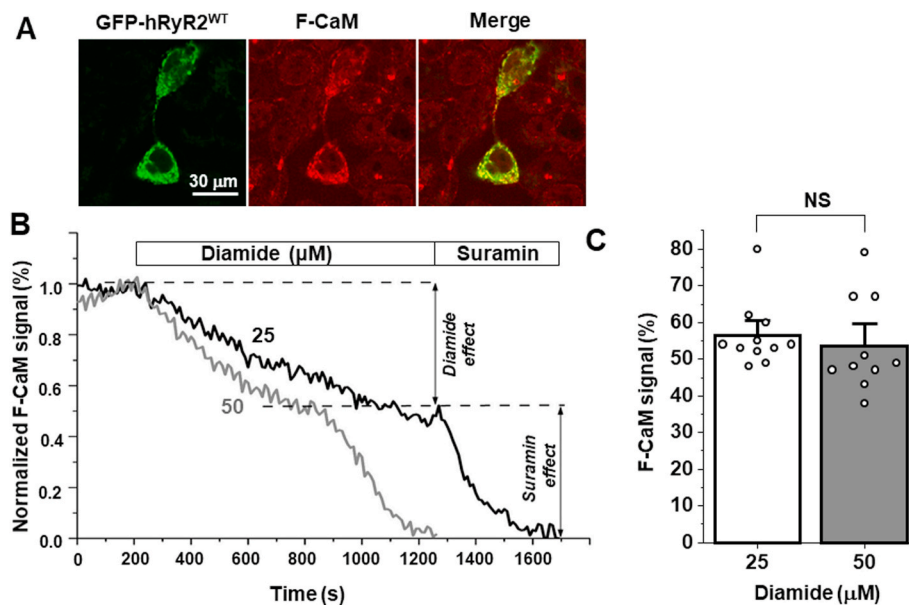


**Fig. 3.** Effect of diamide on CaM dissociation from hRyR2<sup>WT</sup>. **A**, representative images of HEK293 cells expressing GFP-hRyR2<sup>WT</sup> (left), the Alexa 568-labeled CaM (F-CaM) signal (middle) and the merged GFP-hRyR2<sup>WT</sup> and F-CaM signals (right). **B**, representative traces of F-CaM dissociation from GFP-hRyR2<sup>WT</sup> upon application of 25 μM and 50 μM diamide. At the end of the experiment, suramin was applied to completely remove the F-CaM from hRyR2. **C**, Effect of diamide on the CaM dissociation from the hRyR2<sup>WT</sup> complex. On average, levels of the CaM dissociation induced by 25 μM (n = 11 cells) and 50 μM (n = 10 cells) diamide were not significantly different (p = 0.57).

experiments were conducted without adding exogenous CaM to permeabilized cells, the observed effect of diamide on ER Ca<sup>2+</sup> release did not require CaM-hRyR2 interaction.

### 3.3. Effect of oxidative stress on the CaM dissociation from hRyR2

It has been shown that oxidative stress reduces CaM binding to the RyR2 macromolecular complex in cardiomyocytes [23]. Here, we asked whether the level of cross-linking correlates with the degree of CaM dissociation from hRyR2. To measure the diamide effect on CaM-hRyR2 binding, GFP-hRyR2 expressed in HEK293 cells were saturated with 300 nM Alexa-568 labeled CaM (F-CaM) after membrane permeabilization. Cells were then equilibrated with 60 nM F-CaM, corresponding to the physiological concentration of free CaM in cardiomyocytes [34]. The F-CaM signal co-localized with GFP-hRyR2, suggesting a formation of the CaM-hRyR2 complex (Fig. 3A). The Alexa-568 signal was not detected in cells that did not express hRyR2, suggesting that hRyR2a represents the vast majority of CaM binding in our cell model. The application of diamide caused CaM dissociation from hRyR2, which was measured as a relative decline in F-CaM fluorescence over time (Fig. 3B). Overall, 25 and 50 μM diamide decreased the F-CaM signal by  $43.7 \pm 2.7\%$  (n = 11) and  $46.4 \pm 4.1\%$  (n = 10), respectively. Although 50 μM diamide dissociated F-CaM at a higher rate, the final level of F-CaM

signal was the same for both diamide concentrations (Fig. 3C). These results indicate that the degree of oxidative stress producing the maximal hRyR2 cross-linking also resulted in the maximal CaM dissociation from hRyR2.

Role of cysteine 3602 in hRyR2 cross-linking and functional response to oxidative stress.

Cysteine 3635 (C3635) in RyR1 has been shown to undergo functionally important redox modifications, including intersubunit cross-linking [25,26]. Given the high level (~65%) of homology between RyR1 and RyR2 [35], we tested whether the corresponding cysteine 3602 (C3602) in hRyR2 is involved in intersubunit cross-linking. CaM binding site is highly conserved in RyR1 and RyR2 (Fig. 2A Sup). According to recent cryo-EM 3D reconstruction of Ca<sup>2+</sup>-CaM bound to RyR [36,37], cysteine residues that correspond to C3635 in RyR1 and C3602 in hRyR2 are oriented similarly in the CaM binding site (Fig. 2B Sup), suggesting similar functional properties. C3602 was mutated to alanine to generate GFP-hRyR2<sup>C3602A</sup>. Then, Western blot analysis was employed to determine whether the C3602A mutation prevents the diamide-induced cross-linking. Similar to hRyR2<sup>WT</sup>, 25 μM diamide produced the full disappearance of the monomeric form of hRyR2<sup>C3602A</sup>, indicating 100% channel cross-linking (Fig. 4A). The functional response of hRyR2<sup>C3602A</sup> to oxidative stress was tested in the HEK293 cell model. Cells expressing the hRyR2<sup>C3602A</sup> mutant together with

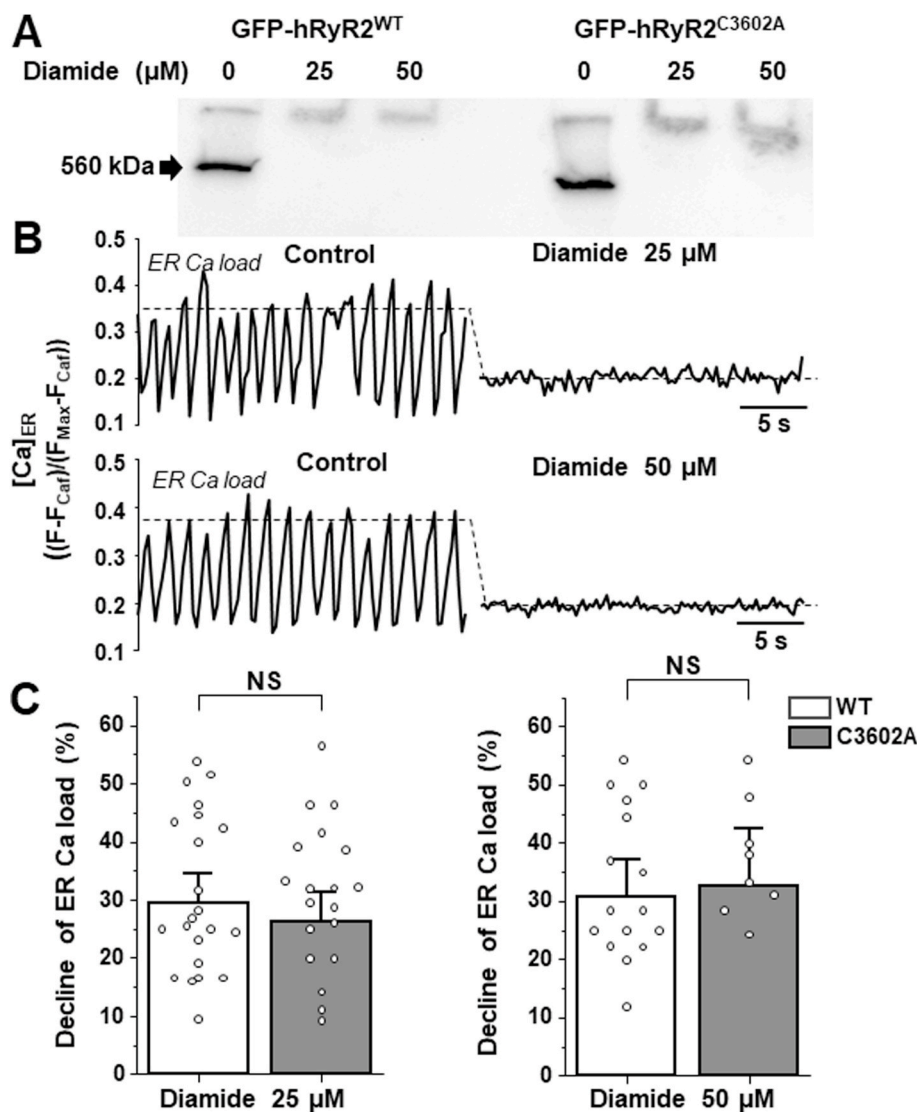


**Fig. 4.** Effect of diamide on the channel's cross-linking,  $\text{Ca}^{2+}$  waves and ER  $\text{Ca}^{2+}$  load in cells expressing hRyR2<sup>C3602A</sup>. **A**, Western blot images of the channel's cross-linking induced by increasing concentrations of diamide in cells expressing hRyR2<sup>WT</sup> and hRyR2<sup>C3602A</sup>. **B**, representative recordings of  $\text{Ca}^{2+}$  waves from two different cells expressing hRyR2<sup>C3602A</sup> (top and bottom) in the control conditions (left) and during 25  $\mu\text{M}$  or 50  $\mu\text{M}$  diamide application (right). The dashed lines indicate the level of ER  $\text{Ca}^{2+}$  load. **C**, diamide-induced depletion of ER  $\text{Ca}^{2+}$  load in cells expressing hRyR2<sup>WT</sup> and hRyR2<sup>C3602A</sup>. On average, changes in ER  $\text{Ca}^{2+}$  load induced by diamide in hRyR2<sup>WT</sup> and hRyR2<sup>C3602A</sup> cells were not significantly different (for 25  $\mu\text{M}$  diamide  $p = 0.49$ ,  $n = 26$  and 22 cells and for 50  $\mu\text{M}$  diamide  $p = 0.81$ ,  $n = 17$  and 9 cells).

SERCA2a generated regular  $\text{Ca}^{2+}$  waves (Fig. 4B) with similar properties as cells with hRyR2<sup>WT</sup> (Fig. 2A). Treatment of the hRyR2<sup>C3602A</sup> expressing cells with diamide decreased ER  $\text{Ca}^{2+}$  load and abolished  $\text{Ca}^{2+}$  waves (Fig. 4B). Overall, 25 and 50  $\mu\text{M}$  diamide decreased ER  $\text{Ca}^{2+}$

load by  $26.2 \pm 3.5\%$  ( $n = 22$ ) and  $32.6 \pm 4.2\%$  ( $n = 9$ ) in cells expressing hRyR2<sup>C3602A</sup>, respectively. These diamide-induced changes in ER  $\text{Ca}^{2+}$  load were not significantly different for hRyR2<sup>C3602A</sup> vs hRyR2<sup>WT</sup> (Fig. 4C). These results strongly suggest that unlike the equivalent

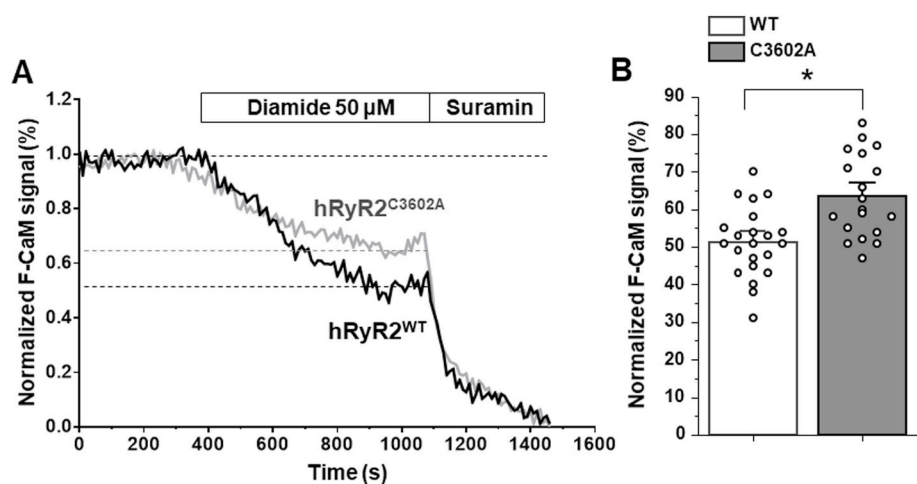


**Fig. 5.** Effect of diamide on the CaM dissociation from hRyR2<sup>C3602A</sup>. **A**, representative traces of F-CaM dissociation from GFP-RyR2 upon application of 50  $\mu\text{M}$  diamide in cells expressing hRyR2<sup>WT</sup> and hRyR2<sup>C3602A</sup>. Suramin was applied to completely dissociate the F-CaM from hRyR2. **B**, effect of diamide on CaM dissociation from hRyR2<sup>WT</sup> and hRyR2<sup>C3602A</sup>. On average, the C3602A mutation reduced diamide-induced CaM dissociation from hRyR2 by 24% ( $p = 0.002$ ; hRyR2<sup>WT</sup>  $n = 22$  and hRyR2<sup>C3602A</sup>  $n = 19$  cells).

cysteine in RyR1, C3602 participates neither in hRyR2 cross-linking nor in hRyR2 activation during oxidative stress.

### 3.4. Role of cysteine 3602 in the regulation of hRyR2 by CaM

Since C3602 is located within the CaM binding domain, we examined whether the C3602A mutation prevents CaM dissociation from hRyR2 during oxidative stress. CaM dissociation from the hRyR2<sup>C3602A</sup> mutant was measured in the presence of 50  $\mu\text{M}$  diamide (Fig. 5A) using an approach similar to that described in Fig. 3. These experiments revealed that the C3602A mutation does not affect CaM binding to hRyR2<sup>C3602A</sup> in the control conditions (measured as the F-CaM signal before the diamide application) and prevents the diamide-induced CaM dissociation by  $\sim 24\%$  (Fig. 5B). Then, we examined whether the C3602A mutation alters the inhibitory effect of CaM on hRyR2-mediated  $\text{Ca}^{2+}$  release.  $\text{Ca}^{2+}$  waves in cells expressing hRyR2<sup>WT</sup> or hRyR2<sup>C3602A</sup> were recorded under control conditions and after adding 1  $\mu\text{M}$  of exogenous CaM (Fig. 6A). In both experimental groups, CaM decreased Ca wave frequency, increased  $\text{Ca}^{2+}$  wave termination level and increased ER Ca load (Fig. 6B). However, the effect of CaM on ER  $\text{Ca}^{2+}$  load and  $\text{Ca}^{2+}$  wave frequency was significantly stronger in hRyR2<sup>C3602A</sup> expressing cells, suggesting that the C3602A mutation enhances the CaM inhibitory action. The subsequent application of 50  $\mu\text{M}$  diamide decreased ER  $\text{Ca}^{2+}$  load by  $29 \pm 3\%$  ( $n = 23$ ) in hRyR2<sup>WT</sup> and by  $19 \pm 3\%$  ( $n = 23$ ) in hRyR2<sup>C3602A</sup> expressing cells. These results indicate that C3602 can be involved in the regulation of hRyR2 by CaM in the control conditions and during oxidative stress. However, the limited protective effect ( $\sim 34\%$ ) of the C3602A mutation suggests that other cysteines, outside the CaM binding site, play more important role in the redox-mediated CaM-hRyR2 dissociation.

## 4. Discussion

In the heart, concerted  $\text{Ca}^{2+}$  release through RyR2 is the essential step for initiating a robust myocardial contraction. Consequently, defects in RyR2 regulation cause contractile dysfunction in a variety of cardiac pathologies [7,8]. RyR2 has been characterized as highly sensitive to oxidative stress, with multiple sites that undergo redox modifications, including disulfide intersubunit cross-linking [38]. We have previously shown that the level of RyR2 cross-linking correlates with the degree of SR  $\text{Ca}^{2+}$  leak in rabbit ventricular myocytes [29]. Moreover, myocytes isolated from a rabbit HF model had a significant fraction of the cross-linked RyR2 [18]. However, the functional significance of this redox modification for human RyR2 remains largely unknown. We

developed a simple expression system to study the redox regulation of hRyR2 in a well-controlled live-cell system that mimics aspects of cardiac  $\text{Ca}^{2+}$  handling. HEK293 cells can be easily transfected with large cDNA plasmids. Also, an advantage of the HEK cell line is that it lacks endogenous RyR, thereby permitting the study of only recombinant RyR2. This system, however, has its own limitations. Although we reconstructed cardiac-like  $\text{Ca}^{2+}$  handling by adding SERCA2a and CaM to the system, some mechanisms of RyR2 regulation are missing (e.g. phosphorylation). In addition, the dyadic organization of  $\text{Ca}^{2+}$  handling cannot be recapitulated in the expressing cell system. Despite these limitations, studies of recombinant human RyR2 provide important insights into the channel structure-function relationships that can uniquely inform therapeutic development targeting a range of serious clinical indications promoted by dysregulated  $\text{Ca}^{2+}$  [39].

In this study, we showed that hRyR2 recombinantly expressed in HEK293 cells undergoes intersubunit cross-linking during diamide exposure (Fig. 1A). The reducing agent DTT restored the monomeric pattern of hRyR2, confirming the reversibility of this redox modification. We compared the sensitivity of hRyR2 cross-linking to cysteine oxidation within the roGFP sensor. By fusing roGFP to the N-terminus of ER transmembrane protein PLB, we were able to measure the level of oxidative stress at the cytosolic side of ER next to hRyR2 (Fig. 1B). In permeabilized cells expressing hRyR2<sup>WT</sup>, 25  $\mu\text{M}$  diamide caused 100% hRyR2 cross-linking that corresponded only to 70% oxidation of roGFP-PLB cysteines (Fig. 1D). It appears that cysteines involved in the RyR2 intersubunit cross-linking are highly sensitive to oxidative stress. While a structural basis for such high sensitivity of the cross-linked cysteines is unclear, it is possible that these RyR2 cysteines are more exposed to the cytosolic milieu, and thus more accessible to the oxidizing agent, than the cysteines in the roGFP-PLB biosensor.

To characterize the link between hRyR2 cross-linking and the channel's function, we studied the effect of diamide on hRyR2-mediated  $\text{Ca}^{2+}$  release (Fig. 2). Expression of both hRyR2 and SERCA2a in HEK293 cells creates a  $\text{Ca}^{2+}$  release/uptake machinery that generates "cardiac-like"  $\text{Ca}^{2+}$  waves [31]. Diamide decreased ER  $\text{Ca}^{2+}$  load followed by the cessation of  $\text{Ca}^{2+}$  waves. As a certain  $[\text{Ca}^{2+}]_{\text{ER}}$  is required to trigger spontaneous CICR, the disappearance of  $\text{Ca}^{2+}$  waves was a result of ER  $\text{Ca}^{2+}$  load depletion. Since SERCA  $\text{Ca}^{2+}$  uptake is not affected by the diamide concentrations used in this study [31], the decline in ER  $\text{Ca}^{2+}$  load is likely to be mediated by an increase in ER  $\text{Ca}^{2+}$  leak due to hRyR2 oxidation. The maximal effect of diamide on ER  $\text{Ca}^{2+}$  load and  $\text{Ca}^{2+}$  leak correlates with the maximal level of hRyR2 cross-linking, suggesting the functional importance of this redox modification. Since intersubunit dynamics within the RyR tetramer

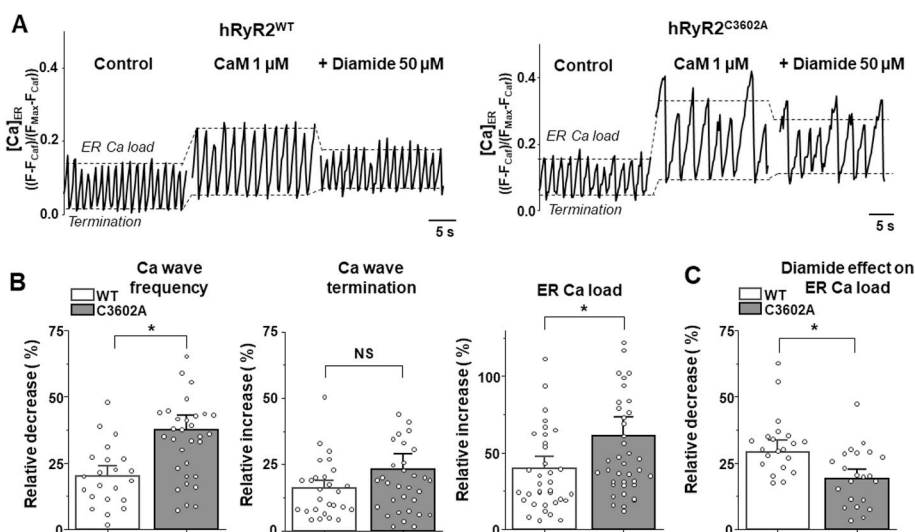


**Fig. 6.** Effects of CaM and diamide on Ca waves and ER  $\text{Ca}^{2+}$  load in cells expressing hRyR2<sup>WT</sup> and hRyR2<sup>C3602A</sup>. **A**, representative recordings of  $\text{Ca}^{2+}$  waves in cells expressing hRyR2<sup>WT</sup> and hRyR2<sup>C3602A</sup> under control conditions, after 1  $\mu\text{M}$  CaM application, and the subsequent application of 50  $\mu\text{M}$  diamide (as indicated). The dashed lines indicate the level of ER  $\text{Ca}^{2+}$  load and  $\text{Ca}^{2+}$  wave termination. **B**, effect of CaM on  $\text{Ca}^{2+}$  wave frequency ( $p = 0.001$ ,  $n = 22$  and  $n = 33$  cells),  $\text{Ca}^{2+}$  waves termination ( $p = 0.15$ ,  $n = 22$  and  $33$  cells) and ER  $\text{Ca}^{2+}$  load ( $p = 0.03$ ,  $n = 36$  and  $40$  cells) in hRyR2<sup>WT</sup> and hRyR2<sup>C3602A</sup> expressing cells. **C**, effect of 50  $\mu\text{M}$  diamide on ER Ca load in the presence of CaM in hRyR2<sup>WT</sup> and hRyR2<sup>C3602A</sup> expressing cells. Overall, the C3602A mutation prevented diamide-induced depletion of ER  $\text{Ca}^{2+}$  load by 34% ( $p = 0.011$ ,  $n = 23$  hRyR2<sup>WT</sup> and 23 hRyR2<sup>C3602A</sup> cells).

determines the channel's gating [40–44], it is not surprising that the intersubunit cross-linking has a significant impact on hRyR2 function.

In skeletal RyR1, C3635 has been identified as a key residue involved in redox regulation [25,27]. This cysteine is located within the CaM binding domain and can participate in intersubunit cross-linking. To evaluate a role of the corresponding C3602 in hRyR2 cross-linking, we analyzed the sensitivity of the hRyR2<sup>C3602A</sup> mutant to diamide oxidation. We found that the C3602A mutation does not protect from hRyR2 cross-linking nor hRyR2 activation by diamide (Fig. 4). In agreement with these findings, recent structural studies suggest that C3602 is too far from a neighboring RyR2 subunit to form a disulfide bond within the RyR2 tetramer [37]. It appears that other sites within hRyR2 are responsible for the formation of intersubunit disulfide bonds. The cross-linking sites might include cysteines in the N-terminal and the central domains. For example, the N-terminus of RyR2 has been reported to be involved in the redox-sensitive tetramer formation [45]. In addition to C3635 in RyR1, 11 other cysteines have been shown to undergo endogenous and exogenous redox modifications [25]. Among these cysteines, C36, C2326 and C2363 can be oxidized to disulfide bonds [25]. While there is no homologue of C2326 in hRyR2, our pilot studies revealed that C36 and C2363 (corresponding C36 and C2330 in hRyR2) are not involved in intersubunit cross-linking (Fig. 3 Sup). Therefore, despite 65% homology, RyR1 and RyR2 display fundamental differences in mechanisms of redox regulation.

The CaM-RyR2 interaction plays an important role in regulation of CICR. CaM binds tightly to each RyR2 subunit and inhibits RyR2 activity via a Ca<sup>2+</sup>-dependent mechanism [46]. It has been shown that oxidative stress can increase SR Ca<sup>2+</sup> leak in ventricular myocytes in part by displacing CaM from the RyR2 complex [22,23]. In the present study, we found that the diamide concentration producing maximal hRyR2 cross-linking resulted in the maximal CaM dissociation from hRyR2 (Fig. 3). Since diamide interacts mainly with cysteine thiol groups (which are absent in CaM), the observed effect was probably mediated by hRyR2 oxidation. The C3602A mutation prevented the diamide-induced CaM dissociation only by ~24% (Fig. 5), indicating that C3602 oxidation has a limited role in this effect. These results suggest that conformational changes within the hRyR2 tetramer caused by the cross-linking (outside of the CaM binding site) play an important role in CaM dissociation from hRyR2. We found that, under control conditions, CaM decreased hRyR2-Ca<sup>2+</sup> release by promoting early CICR termination and by delaying CICR activation (Fig. 6). As a result of hRyR2 inhibition, CaM increased ER Ca<sup>2+</sup> load. The diamide-induced hRyR2 oxidation increased ER Ca<sup>2+</sup> leak and depleted ER Ca load in part by reducing the CaM inhibitory action. As expected based on the CaM binding experiments (Fig. 5), C3602 played only a limited role in the diamide-induced hRyR2 activation.

Collectively, these studies reveal a previously unknown mechanism of human RyR2 regulation. hRyR2 oxidation increases ER Ca<sup>2+</sup> release/leak via at least two main mechanisms: (1) by promoting CaM dissociation due to intersubunit cross-linking and C3602 oxidation and (2) by direct activation of hRyR2 due to intersubunit cross-linking. This is in addition to CaM methionine oxidation, which can also contribute to ER Ca<sup>2+</sup> leak by reducing the CaM binding to RyR [23,47,48].

#### Author contributions

R.N. E.B., D.D.T., R.L.C and A.V.Z. contributed to the conception and design of the study. R.N., E.B., D.K. and R.T.R performed the experimental work and analysis of results. R.N., E.B., D.D.T., R.L.C and A.V.Z. contributed to writing of the manuscript. All authors have approved the version to be published.

#### Declaration of competing interest

The authors declare that there is no conflict of interest regarding the publication of this article.

#### Acknowledgment

This work was supported by the National Institutes of Health Grants HL130231 (to A.V.Z.), HL092097 and HL138539 (to R.L.C), and AG026160 (to D.D.T.). This study was also supported by a James DePauw pilot grant, Loyola University Chicago (to A.V.Z.). The authors would like to thank Dr. Christopher George (University of Cardiff, UK) for providing the vector encoding the GFP-hRyR2 and Dr. Ino for donating the R-CEPIA1er vector.

#### Appendix A. Supplementary data

Supplementary data to this article can be found online at <https://doi.org/10.1016/j.redox.2020.101729>.

#### References

- [1] R. Coronado, J. Morrisette, M. Sukhareva, D.M. Vaughan, Structure and function of ryanodine receptors, *Am. J. Physiol. Cell Physiol.* (1994), <https://doi.org/10.1152/ajpcell.1994.266.6.c1485>.
- [2] G. Meissner, Ryanodine receptor/Ca<sup>2+</sup> release channels and their regulation by endogenous effectors, *Annu. Rev. Physiol.* (1994), <https://doi.org/10.1146/annurev.ph.56.030194.002413>.
- [3] A. Fabiato, Calcium-induced release of calcium from the cardiac sarcoplasmic reticulum, *Am. J. Physiol.* 245 (1983) C1–14.
- [4] D.M. Bers, Cardiac excitation-contraction coupling, *Nature* 415 (2002) 198–205, <https://doi.org/10.1038/415198a>.
- [5] T.R. Shannon, K.S. Ginsburg, D.M. Bers, Quantitative assessment of the SR Ca<sup>2+</sup> leak-load relationship, *Circ. Res.* 91 (2002) 594–600, <https://doi.org/10.1161/01.RES.0000036914.12686.28>.
- [6] A.V. Zima, E. Bovo, D.M. Bers, L.A. Blatter, Ca<sup>2+</sup> spark-dependent and -independent sarcoplasmic reticulum Ca<sup>2+</sup> leak in normal and failing rabbit ventricular myocytes, *J. Physiol.* 588 (2010) 4743–4757, <https://doi.org/10.1113/jphysiol.2010.197913>.
- [7] M. Yano, Ryanodine receptor as a new therapeutic target of heart failure and lethal arrhythmia, *Circ. J.* 72 (2008) 509–514. [JST.JSTAGE/circj/72.509 \[pii\]](https://doi.org/10.1253/circj.72.509).
- [8] L.M. Blayney, F.A. Lai, Ryanodine receptor-mediated arrhythmias and sudden cardiac death, *Pharmacol. Ther.* 123 (2009) 151–177, <https://doi.org/10.1016/j.pharmthera.2009.03.006>.
- [9] S.G. Priori, S.R.W. Chen, Inherited dysfunction of sarcoplasmic reticulum Ca<sup>2+</sup> handling and arrhythmogenesis, *Circ. Res.* 108 (2011) 871–883, <https://doi.org/10.1161/CIRCRESAHA.110.226845>.
- [10] Y.J. Suzuki, G.D. Ford, Redox regulation of signal transduction in cardiac and smooth muscle, *J. Mol. Cell. Cardiol.* 31 (1999) 345–353, <https://doi.org/10.1006/jmcc.1998.0872>.
- [11] A.V. Zima, L.A. Blatter, Redox regulation of cardiac calcium channels and transporters, *Cardiovasc. Res.* 71 (2006) 310–321, <https://doi.org/10.1016/j.cardiores.2006.02.019>.
- [12] L.C. Hool, B. Corry, Redox control of calcium channels: from mechanisms to therapeutic opportunities, *Antioxidants Redox Signal.* 9 (2007) 409–435, <https://doi.org/10.1089/ars.2006.1446>.
- [13] L. Xu, Activation of the cardiac calcium release channel (ryanodine receptor) by poly-S-nitrosylation, *Science* 279 (1998) 234–237, <https://doi.org/10.1126/science.279.5348.234>.
- [14] P. Donoso, G. Sánchez, R. Bull, C. Hidalgo, Modulation of cardiac ryanodine receptor activity by ROS and RNS, *Front. Biosci.* 16 (2011) 553–567, <https://doi.org/10.2741/3705>.
- [15] D. Terentyev, I. Györke, A.E. Belevych, R. Terentyeva, A. Sridhar, Y. Nishijima, et al., Redox modification of ryanodine receptors contributes to sarcoplasmic reticulum Ca<sup>2+</sup> leak in chronic heart failure, *Circ. Res.* 103 (2008) 1466–1472, <https://doi.org/10.1161/CIRCRESAHA.108.184457>.
- [16] A.E. Belevych, D. Terentyev, S. Viatchenko-Karpinski, R. Terentyeva, A. Sridhar, Y. Nishijima, et al., Redox modification of ryanodine receptors underlies calcium alternans in a canine model of sudden cardiac death, *Cardiovasc. Res.* 84 (2009) 387–395, <https://doi.org/10.1093/cvr/cvp246>.
- [17] C.X.C. Santos, N. Anilkumar, M. Zhang, A.C. Brewer, A.M. Shah, Redox signaling in cardiac myocytes, *Free Radic. Biol. Med.* 50 (2011) 777–793, <https://doi.org/10.1016/j.freeradbiomed.2011.01.003>.
- [18] E. Bovo, S.R. Mazurek, A.V. Zima, The role of RyR2 oxidation in the blunted frequency-dependent facilitation of Ca<sup>2+</sup>-transient amplitude in rabbit failing myocytes, *Pflug. Arch. Eur. J. Physiol.* 470 (2018) 959–968, <https://doi.org/10.1007/s00424-018-2122-3>.
- [19] Y. Yan, J. Liu, C. Wei, K. Li, W. Xie, Y. Wang, et al., Bidirectional regulation of Ca<sup>2+</sup> sparks by mitochondria-derived reactive oxygen species in cardiac myocytes, *Cardiovasc. Res.* 77 (2008) 432–441, <https://doi.org/10.1093/cvr/cvm047>.
- [20] B.L. Prosser, C.W. Ward, W.J. Lederer, X-ROS signaling: rapid mechano-chemo transduction in heart, *Science* (2011) 80, <https://doi.org/10.1126/science.1202768>.
- [21] E. Bovo, S.L. Lipsius, A.V. Zima, Reactive oxygen species contribute to the development of arrhythmogenic Ca<sup>2+</sup> waves during  $\beta$ -adrenergic receptor

- stimulation in rabbit cardiomyocytes, *J. Physiol.* 590 (2012) 3291–3304, <https://doi.org/10.1113/jphysiol.2012.230748>.
- [22] M. Ono, M. Yano, A. Hino, T. Suetomi, X. Xu, T. Susa, et al., Dissociation of calmodulin from cardiac ryanodine receptor causes aberrant Ca<sup>2+</sup> release in heart failure, *Cardiovasc. Res.* 87 (2010) 609–617, <https://doi.org/10.1093/cvr/cvq108>.
- [23] T. Oda, Y. Yang, H. Uchinoumi, D.D. Thomas, Y. Chen-Izu, T. Kato, et al., Oxidation of ryanodine receptor (RyR) and calmodulin enhance Ca release and pathologically alter, RyR structure and calmodulin affinity, *J. Mol. Cell. Cardiol.* 85 (2015) 240–248, <https://doi.org/10.1016/j.yjmcc.2015.06.009>.
- [24] A.A. Voss, J. Lango, M. Ernst-Russell, D. Morin, I.N. Pessah, Identification of hyperreactive cysteines within ryanodine receptor type 1 by mass spectrometry, *J. Biol. Chem.* 279 (2004) 34514–34520, <https://doi.org/10.1074/jbc.M404290200>.
- [25] P. Aracena-Parks, S.A. Goonasekera, C.P. Gilman, R.T. Dirksen, C. Hidalgo, S. L. Hamilton, Identification of cysteines involved in S-nitrosylation, S-glutathionylation, and oxidation to disulfides in ryanodine receptor type 1, *J. Biol. Chem.* 281 (2006) 40354–40368, <https://doi.org/10.1074/jbc.M600876200>.
- [26] C.P. Moore, J.Z. Zhang, S.L. Hamilton, A role for cysteine 3635 of RYR1 in redox modulation and calmodulin binding, *J. Biol. Chem.* 274 (1999) 36831–36834, <https://doi.org/10.1074/jbc.274.52.36831>.
- [27] J. Sun, C. Xin, J.P. Eu, J.S. Stamler, G. Meissner, Cysteine-3635 is responsible for skeletal muscle ryanodine receptor modulation by NO, *Proc. Natl. Acad. Sci. U. S. A.* 98 (2001) 11158–11162, <https://doi.org/10.1073/pnas.201289098>.
- [28] J. Sun, L. Xu, J.P. Eu, J.S. Stamler, G. Meissner, Nitric oxide, NOC-12, and S-nitrosoglutathione modulate the skeletal muscle calcium release channel/ryanodine receptor by different mechanisms: an allosteric function for O<sub>2</sub> in S-nitrosylation of the channel, *J. Biol. Chem.* 278 (2003) 8184–8189, <https://doi.org/10.1074/jbc.M211940200>.
- [29] S.R. Mazurek, E. Bovo, A.V. Zima, Regulation of sarcoplasmic reticulum Ca(2+) release by cytosolic glutathione in rabbit ventricular myocytes, *Free Radic. Biol. Med.* 68 (2014) 159–167, <https://doi.org/10.1016/j.freeradbiomed.2013.12.003>.
- [30] T. Mi, Z. Xiao, W. Guo, Y. Tang, F. Hiess, J. Xiao, et al., Role of Cys 3602 in the function and regulation of the cardiac ryanodine receptor, *Biochem. J.* 467 (2015) 177–190, <https://doi.org/10.1042/BJ20141263>.
- [31] E. Bovo, R. Nikolaienko, S. Bhayani, D. Kahn, Q. Cao, J.L. Martin, et al., Novel approach for quantification of endoplasmic reticulum Ca<sup>2+</sup> transport, *Am. J. Physiol. Heart Circ. Physiol.* (2019), <https://doi.org/10.1152/ajpheart.00031.2019>.
- [32] R.L. Cornea, F. Nitu, S. Gruber, K. Kohler, M. Satzer, D.D. Thomas, et al., FRET-based mapping of calmodulin bound to the RyR1 Ca<sup>2+</sup> release channel, *Proc. Natl. Acad. Sci. U. S. A.* 106 (2009) 6128–6133, <https://doi.org/10.1073/pnas.0813010106>.
- [33] B. Morgan, M.C. Sobotta, T.P. Dick, Free radical biology & medicine measuring E GSH and H<sub>2</sub>O<sub>2</sub> with roGFP2-based redox probes, *Free Radic. Biol. Med.* 51 (2011) 1943–1951, <https://doi.org/10.1016/j.freeradbiomed.2011.08.035>.
- [34] X. Wu, D.M. Bers, Free and bound intracellular calmodulin measurements in cardiac myocytes, *Cell Calcium* 41 (2007) 353–364, <https://doi.org/10.1016/j.ceca.2006.07.011>.
- [35] Y. Hakamata, J. Nakai, H. Takeshima, K. Imoto, Primary structure and distribution of a novel ryanodine receptor/calcium release channel from rabbit brain, *FEBS Lett.* 312 (1992) 229–235, [https://doi.org/10.1016/0014-5793\(92\)80941-9](https://doi.org/10.1016/0014-5793(92)80941-9).
- [36] A.A. Maximciuc, J.A. Putkey, Y. Shamoo, K.R. MacKenzie, Complex of calmodulin with a ryanodine receptor target reveals a novel, flexible binding mode, *Structure* 14 (2006) 1547–1556, <https://doi.org/10.1016/j.str.2006.08.011>.
- [37] D. Gong, X. Chi, J. Wei, G. Zhou, G. Huang, L. Zhang, et al., Modulation of cardiac ryanodine receptor 2 by calmodulin, *Nature* (2019), <https://doi.org/10.1038/s41586-019-1377-y>.
- [38] A.V. Zima, S.R. Mazurek, Functional impact of ryanodine receptor oxidation on intracellular calcium regulation in the heart, *Rev. Physiol. Biochem. Pharmacol.* 159 (2016) 39–62, [https://doi.org/10.1007/112\\_2016\\_2](https://doi.org/10.1007/112_2016_2).
- [39] A. Kushnir, B. Wajsborg, A.R. Marks, Ryanodine receptor dysfunction in human disorders, *Biochim. Biophys. Acta Mol. Cell Res.* 1865 (2018) 1687–1697, <https://doi.org/10.1016/j.bbamcr.2018.07.011>.
- [40] E.V. Orlova, I.I. Serysheva, M. Van Heel, S.L. Hamilton, W. Chiu, Two structural configurations of the skeletal muscle calcium release channel, *Nat. Struct. Biol.* (1996), <https://doi.org/10.1038/nsb0696-547>.
- [41] C.-C. Tung, P. a Lobo, L. Kimlicka, F. Van Petegem, The amino-terminal disease hotspot of ryanodine receptors forms a cytoplasmic vestibule, *Nature* 468 (2010) 585–588, <https://doi.org/10.1038/nature09471>.
- [42] R. Zalk, O.B. Clarke, A. des Georges, R.A. Grassucci, S. Reiken, F. Mancina, et al., Structure of a mammalian ryanodine receptor, *Nature* 517 (2015) 44–49, <https://doi.org/10.1038/nature13950>.
- [43] A. des Georges, O.B. Clarke, R. Zalk, Q. Yuan, K.J. Condon, R.A. Grassucci, et al., Structural basis for gating and activation of RyR1, *Cell* (2016), <https://doi.org/10.1016/j.cell.2016.08.075>.
- [44] G. Santulli, D. Lewis, A. des Georges, A.R. Marks, J. Frank, Ryanodine receptor structure and function in health and disease, *Subcell. Biochem.* (2018), [https://doi.org/10.1007/978-981-10-7757-9\\_11](https://doi.org/10.1007/978-981-10-7757-9_11).
- [45] S. Zissimopoulos, C. Viero, M. Seidel, B. Cumbes, J. White, I. Cheung, et al., N-terminus oligomerization regulates the function of cardiac ryanodine receptors, *J. Cell Sci.* 126 (2013) 5042–5051, <https://doi.org/10.1242/jcs.133538>.
- [46] Y. Yang, T. Guo, T. Oda, A. Chakraborty, L. Chen, H. Uchinoumi, et al., Cardiac myocyte Z-line calmodulin is mainly RyR2-bound, and reduction is arrhythmogenic and occurs in heart failure, *Circ. Res.* 114 (2014) 295–306, <https://doi.org/10.1161/CIRCRESAHA.114.302857>.
- [47] E.M. Balog, L.E. Norton, R.A. Bloomquist, R.L. Cornea, D.J. Black, C.F. Louis, et al., Calmodulin oxidation and methionine to glutamine substitutions reveal methionine residues critical for functional interaction with ryanodine receptor-1, *J. Biol. Chem.* 278 (2003) 15615–15621, <https://doi.org/10.1074/jbc.M209180200>.
- [48] E.M. Balog, L.E. Norton, D.D. Thomas, B.R. Fruen, Role of calmodulin methionine residues in mediating productive association with cardiac ryanodine receptors, *Am. J. Physiol. Heart Circ. Physiol.* 290 (2006) 794–799, <https://doi.org/10.1152/ajpheart.00706.2005>.